DOI: 10.61782/fa.2025.0533

FORUM ACUSTICUM EURONOISE 2025

LOW-DRAG RAINBOW-TRAPPING FILTERS FOR BROADBAND SOUND DISSIPATION IN A LOW-SPEED DUCTED FLOW

Cedric Maury[1*] **Teresa Bravo**[2] **Fawad Ali**[1]
Daniel Mazzoni[3] **Muriel Amielh**[3]
[1] Laboratory of Mechanics and Acoustics (LMA CNRS), Marseille, France
[2] Institute for Physical and Information Technologies (ITEFI), Spanish National Research Council (CSIC), Madrid, Spain
[3] Institute of Research on Non-Equilibrium Phenomena (IRPHE CNRS), Marseille, France

ABSTRACT

Rainbow-trapping filters (RTFs) have mostly been designed with closed-end terminations to achieve near-unit broadband absorption under acoustic excitation, with applications as shallow wall-treatments in building acoustics or short anechoic terminations. The current study considers opened rib-designed RTFs being traversed by a low-speed grazing flow. The double objective is to design an enhanced silencer able to achieve broadband sound dissipation, e.g. with minute reflection and transmission of the incident wave, while ensuring a low friction factor. A key element is the lining of the interface between the RTF cavity mouths and the flow duct. Micro-perforated panels (MPP) have been chosen that provide holes diameter – holes pitch parameters optimized to determine maximal total dissipation or minimal friction factor. MPPs also contribute to enhance slow sound effects towards lower frequencies than unlined RTFs. Finite Elements (resp. Reynolds Averaged Navier Stokes k-ε) models have been developed to produce acoustic (resp. aerodynamic) design charts with respect to the MPP parameters. A set of MPP parameters has been found that maximizes the aeroacoustic performance of the MPP-RTF silencer. It has been validated against low-speed wind-tunnel experiments that showed an adverse effect of downstream propagation conditions on the wideband dissipative performance of the MPP-RTF.

Keywords: *broadband silencers, micro-perforated panels, aeroacoustic metamaterials, rainbow-trapping filters.*

1. INTRODUCTION

The emergence of acoustic metamaterials has led to the development of sub-wavelength perfect absorbers whose internal geometry can be tailored to achieve the required wideband and/or low-frequency performance [1]. Aeroacoustic, so-called ventilated, metamaterials have been much less studied [2] although their design is highly motivated by the development of soundproof natural ventilation systems or silencers for air-conditioning or automotive exhaust systems.

The current study focuses on the acoustic and aerodynamic properties of axially-graded fully-opened aeroacoustic metamaterials traversed by a low-speed grazing flow. One considers rib-designed rainbow trapping filters with progressive increase of the cavity depths whose mouth is shielded from the flow by (micro-)perforated panels. Insights into the acoustic and drag performance of such silencers under a low-speed flow are provided by analytical and numerical modellings in Sec. 2 and 3, respectively. Experimental verification of these effects are examined in Sec. 4 from low-speed wind-tunnel experiments.

[*] ***Corresponding author***: *cedric.maury@centrale-marseille.fr*

2. AEROACOUSTIC MODELLING

2.1 MPP-shielded rainbow trapping filters

Rainbow trapping filters (RTF) are retarding silencers of rectangular or cylindrical cross-sections, made up of a set of N sidebranch outer cavities of increasing depths $D(x)$ such that

$$D(x)=\frac{H}{2}\left[1-\frac{(-x)^m}{L^m}\right], \qquad (1)$$

with $-L\le x\le 0$, L and H the duct length and height, respectively and $m>0$. One assumes that the RTF silencer is inserted in a duct with a square cross-section duct of height (and width) H. A cross-sectional view of the RTF is sketched in Fig. 1. m is the rate of increase of the cavity depths and is determinant to achieve impedance matching condition over a broad bandwidth at the inlet of the silencer. In the limit of $m\to\infty$, one gets a locally-reacting expansion chamber while $m=0$ corresponds to a rigid rectangular duct without silencer.

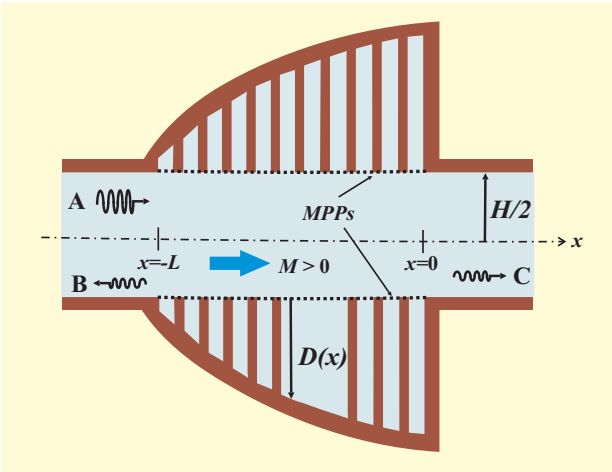

Figure 1. Sketch of a rib-designed rainbow trapping silencer shielded from a low-speed grazing flow of Mach number M (blue arrow) by a micro-perforated panel interface; an incident sound wave propagates along the axial flow.

The power-law increase of the cavity depths when x varies from $-L$ to 0 results in a progressive increase of the wall-admittance monitored by the air cavity stiffness. This produces a slow sound effect [3] with progressive decrease of the acoustic phase speed from c_0 at $x=-L$ down to $c_0/\sqrt{3}$ at $x=0$ where c_0 is the sound speed. The acoustic functionality of a RTF silencer is thus to trap the incident acoustic wave, whose amplitude is denoted A in Fig. 1, and fully dissipate its energy by visco-thermal effects along the inner walls of the cavities. It results in minute reflected and transmitted wave amplitudes, denoted B and C respectively, over the efficiency range of the RTF muffler. If used in transportation sectors, little reflection avoids the occurrence of thermo-acoustic instabilities triggered by acoustic waves back-reflected towards the combustion chamber [4] whereas small transmission contributes to lower noise emissions by thermal engines.

In practice, the entrances of the silencer cavities are shielded from the flow by a perforated or micro-perforated panel (MPP), as sketched in Fig. 1, to prevent clogging by dusts or particle residues, but also to limit the aerodynamic pressure drop when the flow traverses the fully-opened silencer. It will be seen in Sec. 3 that MPPs also have an acoustic functionality, namely to extend the efficiency range of RTF silencers towards the low frequency range.

2.2 Transfer matrix modelling

2.2.1 MPP transfer impedance

The overall transfer impedance, Z_{MPP}, for a MPP with circular holes of diameter d_h and thickness t_h is given by the following expression [5,6] in presence of a low-speed flow with grazing Mach number M

$$\frac{Z_{\text{MPP}}}{\sigma}=\frac{\mathrm{i}\omega\rho_0 t_h}{\sigma}\left[1-\frac{2}{k_h\sqrt{-\mathrm{i}}}\frac{J_1\left(k_h\sqrt{-\mathrm{i}}\right)}{J_0\left(k_h\sqrt{-\mathrm{i}}\right)}\right]^{-1} + \frac{\mathrm{i}\omega\rho_0}{\sigma}\frac{8d_h}{3\pi}F_M + \frac{4}{\sigma}\sqrt{\frac{\eta\rho_0\omega}{2}}+\frac{Z_0}{\sigma}K|M|, \qquad (2)$$

with σ the perforation ratio, η the dynamic viscosity of the air, $k_h=(d_h/2)/r_{\text{visc.}}(\omega)$, the perforate constant, e.g. the ratio of the MPP holes radius to the viscous boundary layer thickness, $r_{\text{visc.}}(\omega)=\sqrt{\eta/\rho_0\omega}$, ρ_0 the air density, ω the angular frequency and $Z_0=\rho_0 c_0$ the air

characteristic impedance. Eq. (2) is valid for linear acoustic regimes and for MPPs with a low perforation ratio, typically lower than 2%, for hole interaction effects to be negligible. Inner viscous dissipation and inertial effects within the MPP holes are accounted for within the first term of Eq. (2) where J_1 and J_0 are Bessel functions of the first kind and orders 1 and 0, respectively. The second term describes the added mass effect at the inlet/outlet of the MPP holes. It is reduced by grazing flow effects, all the more than the flow speed increases, by a correction factor $F_M = \left[1+\left(12.6\,|M|\right)^3\right]^{-1}$. The third term in Eq. (2) accounts for the added resistance at the MPP holes inlet and outlet while the fourth term describes the excess resistance induced at the MPP inlet by the grazing flow. It increases the MPP resistance by $K|M|Z_0/\sigma$, with the value $K=0.15$ educed for $|M|<0.15$ [6].

2.2.2 Transfer matrix model

Assuming plane wave propagation in the duct and in the cavities, an overall transfer matrix can be defined between the inlet ($x=-L$) and outlet ($x=0$) of the MPP-RTF silencer as the following product

$$\mathbf{T}=\prod_{n=1}^{N}\mathbf{T}_n=\begin{bmatrix}T_{11} & T_{12}\\ T_{21} & T_{22}\end{bmatrix}, \tag{3}$$

between the elementary transfer matrices $\mathbf{T}_n$ that relate the acoustic pressure and volume velocity fields [7] across the n$^{\text{th}}$ MPP-cavity-rib units. Each elementary transfer matrix results from the product, $\mathbf{T}_n=\mathbf{T}_d\,\mathbf{T}_t\,\mathbf{T}_{\text{cav},n}$, with $\mathbf{T}_d$ (resp. $\mathbf{T}_t$) the propagating matrices over the cavity width d (resp. the rib thickness t) and $\mathbf{T}_{\text{cav},n.}$ a matrix that describes the wall admittance effect of the n^{th} MPP-cavity. Assuming $\mathrm{e}^{\mathrm{j}\omega t}$ time-dependence, each propagating matrix $\mathbf{T}_w$ reads

$$\mathbf{T}_w=\mathrm{e}^{-\mathrm{j}Mkw}\begin{bmatrix}\cos(kw) & \mathrm{j}y_0^{-1}\sin(kw)\\ \mathrm{j}y_0\sin(kw) & \cos(kw)\end{bmatrix}, \tag{4}$$

with $w=d,t$ the length of each duct unit traversed by a flow with bulk Mach number M, $S=H^2$ the duct cross-sectional area and $y_0=S/Z_0$. The duct wavenumber k in presence of a uniform low-speed flow is given by $k=\left(k_0-\mathrm{j}\mathrm{Fr}M/2H\right)/\left(1-M^2\right)$ in which $k_0=\omega/c_0$. $\mathrm{Fr}=0.0072+0.612\,\mathrm{Re}^{-0.35}$ ($\mathrm{Re}<4.10^5$) is the Froude friction factor that accounts for the dispersion induced by the turbulent flow, and $\mathrm{Re}=MHZ_0/\eta$ is the flow duct Reynolds number.

Coupling between the ducted flow and the nth MPP-cavity is described by the transfer matrix [7]

$$\mathbf{T}_{\text{cav},n}=\frac{1}{1+2MY_{\text{cav},n}y_0}\times\begin{bmatrix}1+MY_{\text{cav},n}y_0 & M^2Y_{\text{cav},n}^2y_0^2\\ Y_{\text{cav},n} & 1+MY_{\text{cav},n}y_0\end{bmatrix}, \tag{5}$$

with $Y_{\text{cav},n}$ the local sidebranch volume admittance of the n^{th} MPP-cavity. It reads $Y_{\text{cav},n}=S_{\text{cav}}\,y(x_n)/Z_0$ with $S_{\text{cav}}=2Hd$ the cavities entrance area and x_n the axial location of the n^{th} sidebranch. The specific admittance is calculated as $y(x_n)=\left[Z_{\text{MPP}}/(Z_0\sigma)-\mathrm{j}\cot(k_0'x_n)\right]^{-1}$ with Z_{MPP}/σ given by Eq. (2) and k_0' a complex frequency-dependent wavenumber that accounts for visco-inertial and thermal effects over each cavity wall following the Johnson-Champoux-Allard-Lafarge model [8].

Assuming that the duct outlet ($x\to+\infty$) is infinite, e.g. there are no back-transmitted wave, as seen in Fig. 1, the following left reflection (resp. left-to-right transmission) coefficients r_{11} (resp. t_{12}) are obtained

$$\begin{cases}r_{11}=\dfrac{(T_{11}+y_0T_{12})-(T_{21}+y_0T_{22})}{(T_{11}+y_0T_{12})+(T_{21}+y_0T_{22})}\\ t_{12}=\dfrac{1+r_{11}}{T_{11}+y_0T_{12}}\end{cases}. \tag{6}$$

On can then deduce the power dissipated by the MPP-RTF silencer, namely $\eta=1-\rho-\tau$ with $\tau=|t_{12}|^2$ the transmission coefficient and $\rho=(1-M)^2|r_{11}|^2/(1+M)^2$ the convected reflection coefficient. The transmission loss (TL) is defined as $\mathrm{TL(dB)}=-10\log_{10}(\tau)$.

3. ACOUSTIC PROPERTIES OF A MPP-RTF

Simulations have been carried out to examine the influence of the MPP holes diameter and flow speed on the

acoustical performance of a MPP-RTF silencer. They have been achieved using the cost-efficient transfer matrix model presented in Sec. 2.2.2. This model has been validated in the no-flow case against finite element visco-thermal acoustic simulations [3], but also against experiments, as shown in Sec. 5.

One considers a MPP-RTF cubic silencer of length $L = 0.15$ m, of square cross-section of height and width $H = W = L$, composed of $N = 15$ cavities of width $d = 7$ mm separated by ribs of thickness $t = 3$ mm. Axial variations of the cavity depths follow Eq. (1). The cavity mouths are covered by a MPP of thickness $t_h = 0.5$ mm, of center-to-center separation $s_h = 5$ mm between the holes whose diameter has been varied to assess its effect on the silencer performance.

3.1 Influence of the MPP holes diameter

Figure 2 shows variations of the fraction of incident power dissipated, reflected and transmitted by MPP-RTF silencers when decreasing the MPP holes diameter from 0.9 mm down to 0.2 mm while keeping a constant holes pitch set to 5 mm. This corresponds to a decrease of the perforation ratio from 2.54% to 0.13%. The performance of the unshielded RTF silencer is also shown. It exhibits a near-unit dissipation plateau, minute reflection and little transmission as from 1 kHz up to the duct cut-on frequency 1140 Hz. Shielding the RTF by a MPP with 0.9 mm holes diameter significantly downshifts the onset of high performance from 1 kHz down to 650 Hz while enlarging by a factor 3.5 the efficiency range of the silencer, that now extends from 650 Hz to 1140 Hz. Over this range, the dissipation exceeds 0.9 and the reflection (resp. transmission) stays below 0.02 (resp. 0.08) respectively. This translates into a TL between 11dB and 18 dB, as shown in Fig. 3. This is due to increased reactance brought by the micro-perforations to the RTF cavity mouths whose resonances are still able to merge due to the added resistance.

Further decreasing the MPP holes diameter increases the extra inertial and resistive effects brought by the MPP holes to the silencer. As observed in Fig. 2, it results in a progressive downshift of the silencer efficiency range towards the low frequency range. It is accompanied by a decrease (resp. increase) of the maximum dissipation (resp. minimum transmission) values, as the holes diameter decreases.

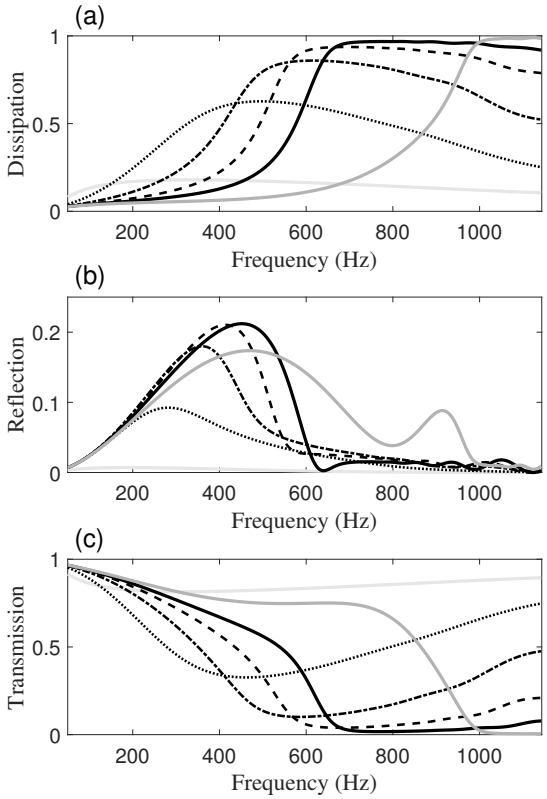

Figure 2. Influence of the MPP holes diameter on the dissipation (a), reflection (b) and transmission (c) coefficients of a MPP-RTF silencer in the no-flow case when decreasing the MPP holes diameter d_h (0.9 mm, plain black; 0.7 mm, dashed black, 0.5 mm, dash-dotted black; 0.4 mm, dotted; 0.2 mm, light grey) and without MPP (plain grey).

Note that variations of the MPP properties hardly influence the minute reflection properties of the MPP-RTF silencer. As for the largest holes diameter, low reflections are due to high dissipation within the cavities. They are due to increased transmission when the holes diameter increases. In the limit of very low perforation ratio (0.13%) with ultra-small holes diameters, almost full transmission is achieved with a TL lower than 1 dB.

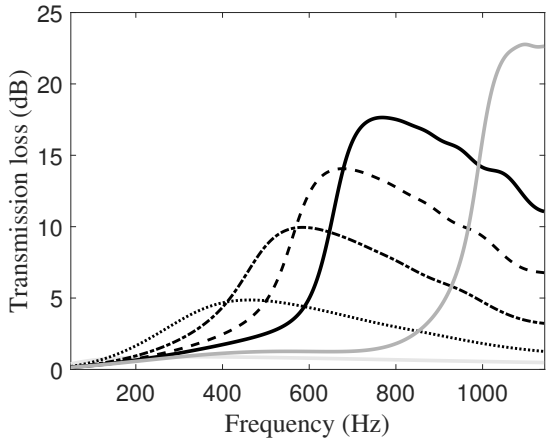

Figure 3. Influence of the MPP holes diameter on the Transmission loss (dB) spectra of a MPP-RTF silencer in the no-flow case when decreasing the MPP holes diameter d_h (0.9 mm, plain black; 0.7 mm, dashed black, 0.5 mm, dash-dotted black; 0.4 mm, dotted; 0.2 mm, light grey) and without MPP (plain grey).

3.2 Low-speed flow effects

In practice, a low-speed flow will travel within the MPP-RTF silencer, as would be the case in a ventilation or an automotive exhaust system. Assuming a discharge flow rate, the sound wave, which propagates from the shallowest to the deepest cavity, will also travel along the flow direction, e.g. under downstream propagation conditions (DPC). The effect of an increasing flow speed on the MPP-RTF acoustical performance has been simulated in Fig. 4. Simulations have been performed on a MPP-RTF silencer assuming a MPP with holes diameter $d_h = 0.9$ mm and holes pitch $s_h = 5$ mm . The main influence is a reduction of the efficiency bandwidth for the dissipation and the transmission loss towards higher frequencies as the flow speed increases. It is accompanied by a decrease of the maximum performance values. The onset of high dissipation values (greater than 0.9) and high TL (greater than 11 dB) is upshifted from 650 Hz (no-flow case) towards 880 Hz (flow at 30 m.s^{-1}). The TL dynamics, 11 dB – 18 dB without flow, reduces to 11 dB – 12 dB with flow at 30 m.s^{-1}. Note that the reflection coefficient is rather unaffected by low-speed flow effects as it stays below 2% over the range of flow speed variations.

Such adverse flow effects are due to an increase of the MPP resistance and a decrease of the MPP reactance, as seen from Eq. (1), when the flow speed or Mach number increases. Such over-resistive and under-reactive conditions could be overcome if integrated in an optimisation process that maximizes the total dissipation of the silencer.

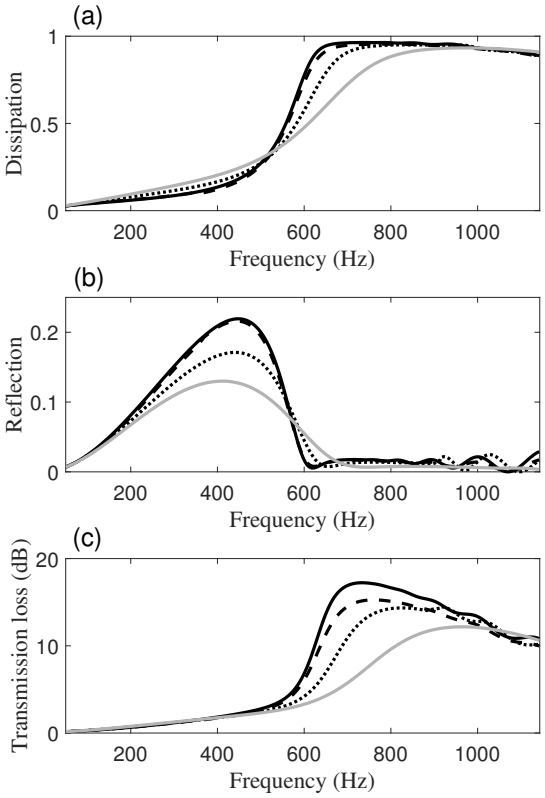

Figure 4. Influence of the flow velocity on the dissipation (a), reflection (b) and transmission loss (c) of a MPP-RTF silencer when traversed by a grazing flow of bulk velocity 10 m.s^{-1} (dashed black), 20 m.s^{-1} (dotted black) and 30 m.s^{-1} (grey); also shown the no-flow case (plain black).

4. AERODYNAMIC PERFORMANCE

Shielding the RTF silencer cavities from a grazing flow by using MPPs not only has an acoustic functionality, as seen in Sec. 3.1, but also limits the pressure drop that would be induced by interaction between the flow and the RTF cavity

mouths through detachment, vortex shedding and re-attachment at the cavity edges. A quantifier of this effect is the friction factor of the cubic MPP-RTF silencer that takes the following form, with $H = L$,

$$\varphi = \frac{H}{L}\frac{\Delta p}{\rho_0 U^2} = \frac{\Delta p}{\rho_0 U^2}, \qquad (7)$$

with Δp the pressure drop across the axial length L of the silencer and U the mean flow speed. These quantities have been calculated from Reynolds Averaged Navier Stokes k-ε model [9] solved by Finite Volume in Ansys Fluent imposing a fully-developed turbulent boundary layer profile at the silencer inlet with outer velocity 30 m.s^{-1} and turbulence rate 2%, typical of low-speed wind-tunnels.

Figure 5 shows a substantial decay of the friction factor when increasing the MPP holes pitch from 0.5 mm to 5 mm. It amounts to 17% for ultra small (0.2 mm) and 14.5% for near-millimetric (0.9 mm) holes diameters. This is associated to a decrease of the perforation ratio from 12.57% to 0.13% in the former case, and from 63.62% to 2.54% in the latter case. Moreover, the friction factor for $d_h = 0.9$ mm stays consistently higher than that for $d_h = 0.2$ mm, by 1 to 4%. As for $d_h = 0.9$ mm, holes pitch values lower than d_h have been excluded.

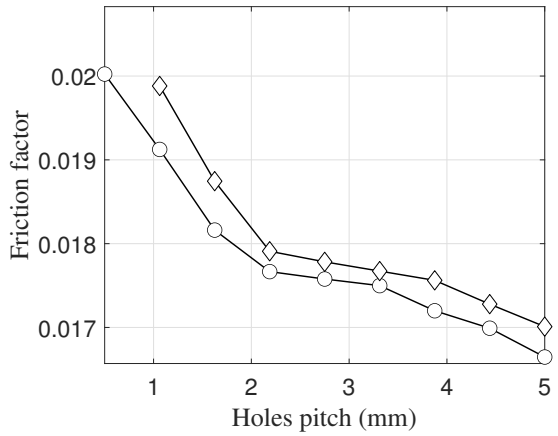

Figure 5. Influence of the MPP holes pitch on the friction factor of a MPP-RTF silencer traversed by a low-speed flow of bulk velocity 30 m.s^{-1} for two MPP holes diameters ($d_h = 0.2$ mm, circles; ($d_h = 0.9$ mm, diamonds).

It appears that the MPP with the lowest friction factor is the one with the smallest holes diameters and the largest holes pitch, e.g. with a very low perforation ratio. Back to Fig. 2 (light grey curves), it is associated to poor dissipation and transmission properties. A compromise thus has to be found to achieve both acceptable acoustical and aerodynamic performance. It can be seen from Fig. 5 that a MPP with holes pitch greater than 2 mm and holes diameter of 0.9 mm (for ease of manufacture) ensures a friction factor below 0.018. Assuming a holes pitch of 5 mm, Fig. 2 shows it provides excellent acoustical performance in the no-flow case, that should however be moderated by the results of Fig. 4 under a low-speed flow at 30 m.s^{-1}.

5. EXPERIMENTAL VERIFICATION

Low-speed wind-tunnel experiments have been performed to verify the simulated acoustical performance of a cubic RTF silencer of length, width and height $L = W = H = 0.15$ m, additively manufactured in ABS material. The silencer is shielded from a low-speed flow (30 m.s^{-1}) by a perforated panel of thickness 1.5 mm, holes diameter 2.6 mm and perforation ratio 2.8%. The RTF is composed of 20 cavities of width 3.5 mm separated by ribs of thickness 4 mm. Figure 6 shows that the silencer is plugged onto a low-speed wind-tunnel duct section. During the measurements, the inlet and outlet of the silencer are prolonged by 1 m length rigid square duct sections to ensure flow channeling. The airflow is generated by a centrifugal fan insulated with mufflers, straightened by honeycomb panels in a settling chamber, then accelerated through a convergent towards the test section. A transitional, almost turbulent, boundary layer has been characterized from hot-wire measurements at the silencer inlet location.

The test section is instrumented in order to measure the scattering matrix of the silencer [10]. Two sources and two pairs of three boundary layer microphones are located respectively in the 1 m duct sections upstream and downstream the silencer. The sources are sequentially driven by white noise to generate two independent states within the duct test section. The associated outgoing and ingoing plane wave amplitudes are deduced from the transfer functions measured between the microphones and the source drive signals after pseudo-inversion of the plane wave propagation matrix that accounts for convective effects and visco-thermal losses in presence of flow up to the duct cut-on frequency 1140 Hz. The scattering matrix

gathers the outgoing and ingoing wave amplitudes for each acoustic state from which the dissipation, reflection and transmission coefficients are readily deduced.

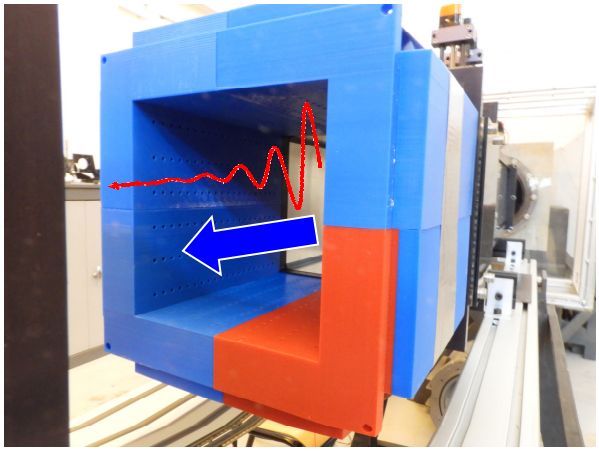

Figure 6. Photography of the outlet of a square RTF silencer mounted on a low-speed wind-tunnel and shielded from the grazing flow by perforated panels; the blue (resp. red) arrows represent the flow (resp. sound wave) travelling through the silencer.

It can be seen from Fig. 7 that the Finite Element simulations and the scattering matrix measurements closely correlate, showing high dissipation values of the perforated-RTF silencer exceeding 0.9 from 650 Hz to 950 Hz in the no-flow case. Over this range, merging occurs between the resonances of the activated perforate-RTF cavities. It is associated to very small values of the reflection coefficient, below 0.02, and a low transmission coefficient that stays below 0.2.

Without perforated coating, it is found from simulations (not shown) that the RTF silencer produces a high dissipation plateau only above 1400 Hz, beyond the plane wave regime that extends up to 1140 Hz. Adding the perforated coating over the RTF cavities thus downshifts by 750 Hz the onset of high acoustical performance. This is due to inertial effects added by the perforates with 2.8% wall porosity. Because of limitations on the minimum holes diameter that can be printed from fused deposition modelling using ABS polymer, such low-perforation ratio was achieved by increasing the perforate holes pitch, 7.5 mm along the streamwise direction and 25 mm along the spanwise direction, as seen from Fig. 6, rather than by decreasing the holes diameter to small sub-millimetric values. Due to the supra-millimetric holes diameters, visco-thermal dissipation occurs essentially within the RTF cavities. It well manages to balance the reflection and transmission leakages around 750 Hz, but slightly over-resistive conditions are observed above 900 Hz. They produce a progressive decrease of the dissipation down to 0.8 as well as an increase of the transmission up to 0.2 when the frequency raises up to 1100 Hz.

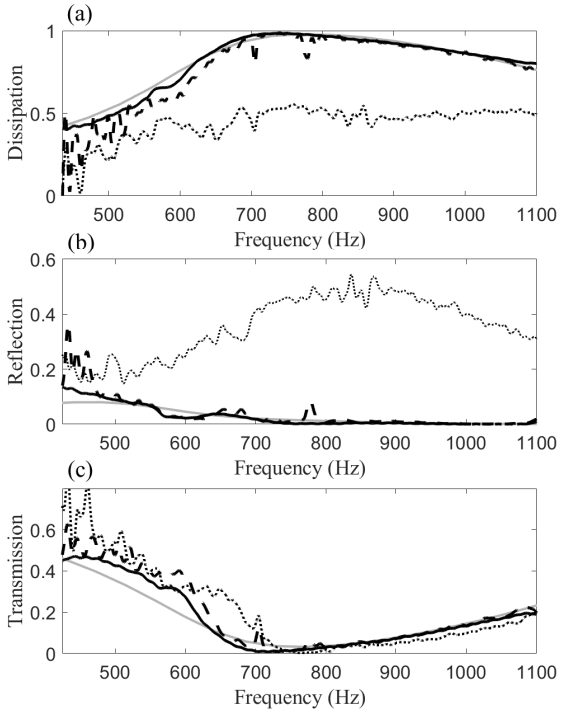

Figure 7. Dissipation (a), reflection (b) and transmission (c) spectra of the perforated RTF silencer simulated by Finite Element method (grey) and measured (black) in the no-flow case and under a low-speed flow at 30 m.s^{-1} assuming upstream (dashed) or downstream (dotted) plane wave excitations.

Under a low-speed flow (30 m.s^{-1}), one observes a slight upshift of the onset of high dissipation and transmission performance, from 650 Hz without flow to 690 Hz with flow, with almost unchanged reflection properties. This trend is in accordance with the low-speed flow effects simulated by the transfer matrix model in Fig. 4. These effects are due to the added resistance and deficit in wall

reactance caused by the flow. However, they appear to be less pronounced with respect to the effect of the same flow speed over a MPP-coated RTF silencer, as seen when comparing Fig. 7 and Fig. 4.

Assuming an incident wave propagating against the flow, e.g. impinging the silencer from the outlet side, Fig. 7 shows that it produces moderate broadband dissipation (that stays around 0.5) due to back reflections (up to 50% of the incident power). This is due to the wall admittance discontinuity encountered by the wave when entering the silencer flow outlet due to the low stiffness of the deepest cavity. This breaks the impedance matching condition that would be satisfied by the wave if it was entering the silencer flow inlet, due to the high stiffness of the shallowest cavity and progressive increase of the wall admittance. One also note from Fig. 7(c) the absence of reciprocity in transmission under grazing flow conditions.

6. CONCLUSIONS

The acoustic and aerodynamic effect of covering the cavities of RTF silencers by MPP or perforated panels has been examined under no-flow and low-speed grazing flow conditions, up to Mach 0.087. Transfer matrix modelling and measurements of the scattering matrix in a low-speed wind tunnel showed robustness of the broadband low-reflection and high dissipation performance to grazing flow effects, albeit over a bandwidth that reduces as the flow speed increases. The transmission loss of the coated RTF silencer is especially sensitive to this adverse flow effect.

A trade-off has to be found on the MPP parameters to ensure both high dissipation performance and low friction factor since either objective requires concurrent parameter sets. Further coupled acoustic and computational fluid dynamic simulations should be performed at the MPP holes local scale to investigate the geometrical parameters favoring visco-thermal dissipation in the acoustic/thermal boundary layers while limiting the occurrence of flow-induced vortex shedding over/within the holes and responsible of the drag. However, the analysis is not straightforward due to the interaction between the near-wall shear layers and the acoustic waves.

7. ACKNOWLEDGMENTS

This work is part of the project PID2022-139414OB-I00 funded by MCIN/AEI/10.13039/501100011033/ and by "ERDF A way of making Europe". It has also received support from the French government under the France 2030 investment plan, as part of the Initiative d'Excellence d'Aix-Marseille Université - A*MIDEX (AMX-22-RE-AB-157).

8. REFERENCES

[1] V. Romero-Garcia and A.-C. Hladky-Hennion (Editors): *Fundamentals and Applications of Acoustic Metamaterials: From Seismic to Radio Frequency*. London: ISTE Ltd, 2019.

[2] G. Palma, H. Mao, L. Burghignoli, P. Göransson and U. Iemma, "Acoustic Metamaterials in Aeronautics," *Applied Sciences*, 971, 8, 2018.

[3] T. Bravo and C. Maury: "Broadband sound attenuation and absorption by duct silencers based on the acoustic black hole effect: Simulations and experiments," *Journal of Sound and Vibration*, 561, 117825, 2023.

[4] T. Poinsot, "Prediction and control of combustion instabilities in real engines," *Proceedings of the Combustion Institute*, 36, 1–28, 2017.

[5] D. Y. Maa, "Potential of micro-perforated panel absorbers," *Journal of the Acoustical Society of America,* 104, 2861–2866, 1998.

[6] S. Allam and M. Åbom, "A new type of muffler based on microperforated tubes," *Journal of Vibration and Acoustics*, 133, 031005, 2011.

[7] M. L. Munjal, "Velocity ratio-cum-transfer matrix method for the evaluation of a muffler with mean flow," *Journal of Sound and Vibration*, vol. 39, pp. 105–119, 1975.

[8] J. F. Allard and N. Attala: *Propagation of Sound in Porous Media: Modelling Sound Absorbing Materials*, 2nd edn. Chichester: John Wiley & Sons Ltd, 2009.

[9] T.-H. Shi, W. W. Liou, A. Shabir, Z. Yang and J. Zhu, "A New k-ε Eddy-Viscosity Model for High Reynolds Number Turbulent Flows – Model Development and Validation," *Computers and Fluids*, 24, 227–238, 1995.

[10] E. Garnell, M. Åbom and G. Banwell, "The use of the two-port method to characterize high-speed small fans," *Applied Acoustics*, 146, 155–163, 2019.